



## Growth and oxidation of aluminum thin films deposited on Ag(1 1 1)

H. Oughaddou\*, S. Vizzini, B. Aufray, B. Ealet, J.-M. Gay, J.-P. Bibérian, F.A. d'Avitaya

*CRMCN-CNRS, Campus de Luminy, Case 913, 13288 Marseille Cedex 09, France*

Received 18 January 2005; received in revised form 24 June 2005; accepted 27 June 2005  
Available online 2 August 2005

### Abstract

Auger electron spectroscopy (AES) and low energy electron diffraction (LEED) were used to study the first steps of growth and oxidation of aluminum on Ag(1 1 1) substrate. We find that the growth of aluminum at room temperature (RT) shows the formation of a complete monolayer (ML) in epitaxy with the substrate. After deposition at RT of one aluminum ML, the dissolution kinetics is recorded at 200 °C and the bulk diffusion coefficient is deduced. We also show that the oxidation at RT of one aluminum ML is very rapid, and that both aluminum and oxygen do not dissolve in silver up to 500 °C. From the AES intensities variations, we deduce the composition profile of the oxide layer which corresponds probably to the stacking . . ./Ag/Ag/Al/O.

© 2005 Elsevier B.V. All rights reserved.

Aluminum oxide have been extensively studied in the last years mainly for its technological applications in catalysis [1] and as an insulating barrier in magnetic tunnel junctions [2]. In both cases, the control of the growth of ultrathin oxide films on metallic surfaces is of crucial importance and many studies are done to find how to process well controlled homogenous oxide layers [3–6].

In this paper, we report on the study of the first steps of the formation of aluminum oxide on Ag(1 1 1) substrate. The choice of silver is motivated by future important technological applications. In fact, Ag has

the lowest resistivity (1.47  $\mu\Omega$  cm) [7] among all metals and it could be an alternative for future metallization schemes [8,9]. Aluminum oxides and oxynitrates were also used as a passivation layers for silver [10,11].

The Ag(1 1 1) substrate was cleaned by repeated  $\text{Ar}^+$  ions sputtering cycles ( $5 \times 10^{-5}$  Torr, 600 V) and subsequent annealing at elevated temperatures (400–500 °C) until a sharp  $p(1 \times 1)$  LEED pattern was obtained. Aluminum was deposited onto the substrate at RT from a calibrated effusion cell with a pyrolytic boron nitride crucible at a background pressure of  $2 \times 10^{-10}$  Torr. The sample is alternatively placed in front of the aluminum evaporation cell for a given time, then in front of a CMA Auger spectrometer to

\* Corresponding author. Fax: +33 4 91 82 91 97.  
E-mail address: [Hamid@crmcn.univ-mrs.fr](mailto:Hamid@crmcn.univ-mrs.fr) (H. Oughaddou).

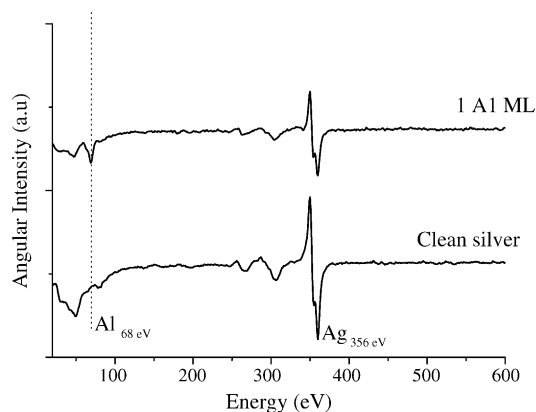


Fig. 1. AES spectra recorded before and after the deposition at RT of one aluminum monolayer.

monitor the surface concentration and then in front of a LEED optics to observe the surface structure. The deposition rate, calibrated from a quartz balance, was 0.25 ML/min (one theoretical dense aluminum ML is  $1.41 \times 10^{15}$  at  $\text{cm}^{-2}$ ). Oxidation process was performed at RT by exposing the sample to a constant pressure of molecular oxygen ( $4 \times 10^{-6}$  Torr) in the chamber.

Fig. 1 shows two AES spectra recorded before and after the deposition at RT of about one aluminum ML. One can observe on the first spectrum that the surface is perfectly clean after sample preparation. On the second spectrum, the aluminum Auger peak appears at 68 eV which corresponds to aluminum atoms in a metallic state without oxygen contamination. Note also, that the silver Auger peak (356 eV) is attenuated by about 40% after aluminum deposition. Using the following equation [12]:

$$I^{\text{Ag}} = I_0^{\text{Ag}} \exp\left(\frac{-d}{\lambda_{(\text{Al})} \cos(\theta)}\right)$$

(where  $I_0^{\text{Ag}}$  and  $I^{\text{Ag}}$  are respectively the AES intensities of silver before and after the aluminum deposit,  $\lambda_{(\text{Al})}$  the inelastic mean free path of Ag Auger electrons through an aluminum film and  $\theta$  ( $42.3^\circ$ ) the entrance angle of the analyzer used) and assuming the thickness of one aluminum monolayer equal to its theoretical value (2.86 Å), we calculate  $\lambda_{(\text{Al})} = 7.5 \pm 0.2$  Å. This value is close to the one determined elsewhere (7 Å) [13].

Moreover, there is no evolution of the LEED pattern during the deposition process, i.e. the  $p(1 \times 1)$

structure is still present after the deposition of one aluminum ML with a weak background increase. These observations indicate the perfect epitaxy of the dense aluminum layer (coverage 1 ML) onto the Ag(1 1 1) surface. This is not unexpected considering that aluminum and silver have the same bulk structure (FCC) with a small mismatch ( $\sim 1\%$ ).

In order to study the role played by the oxidation process on the stability of this aluminum ML, we have followed by AES-LEED the dissolution kinetics of aluminum before and after an oxidation process.

The kinetics displayed on Fig. 2 a shows the time dependence of the peak-to-peak intensities of silver and aluminum Auger signals during the dissolution

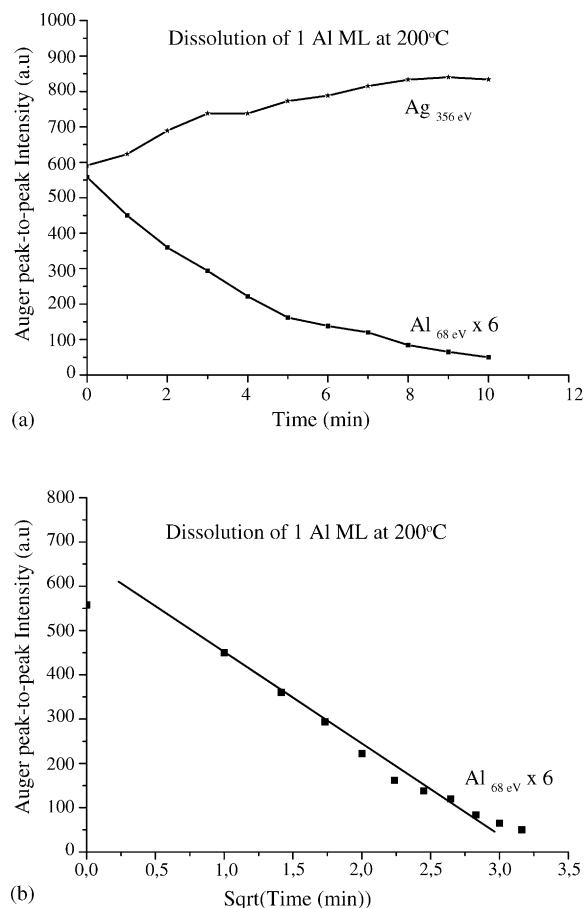


Fig. 2. Dissolution kinetics of one aluminum ML recorded at  $200^\circ\text{C}$ : (a) time dependence of the Auger peak-to-peak intensities of both silver and aluminum and (b) aluminum intensity vs. square root of time. The bulk diffusion coefficient is derived from the slope of the curve.

process at 200 °C of one aluminum ML previously deposited on the Ag(1 1 1) surface at RT. The aluminum Auger signal continuously decreases down to a value close to zero whereas the silver Auger signal increases up to a constant value.

During the first steps of the aluminum dissolution process there is a possible formation of a surface alloy in relation with the order tendency between Al and Ag (cf bulk phase diagram [14]). Nevertheless, because the aluminium diffusion in the bulk of silver is only driven by both bulk diffusion coefficient and the weak solubility of Al in Ag at 200 °C [14], the decrease of the amount of aluminum close to the surface  $C_s(t)$  must follow the classic rule in square root of time

$$C_s(t=0) - C_s(t) = 2C_v(x \simeq 0, t) \sqrt{\frac{Dt}{\pi}} \quad (1)$$

where  $C_v(x \simeq 0, t)$  is the limit of solubility near the surface ( $x \simeq 0$ ) at time  $t$  (i.e. during the dissolution process) and  $D$  the bulk diffusion coefficient.

Taking into account the fact that the amount of aluminum deposited on the surface do not exceed 1 ML, the surface alloy which can be formed, is necessary limited to few atomic planes and the Auger signal intensity is approximatively proportional to the surface concentration  $C_s(t)$ . Fig. 2 b shows a linear decrease of the surface concentration as a function of the square root of time. Assuming that  $C_v(x \simeq 0, t)$  is equal to 8.75 at.% which is the limit of solubility of aluminum in silver at 200 °C [14], the bulk diffusion coefficient  $D$  can be evaluated from the slope of the experimental curve using relation (1). The diffusion coefficient is therefore equal to  $(1.3 \mp 0.2) \times 10^{-16}$  cm<sup>2</sup>/s. This value is 10 times smaller than the one extrapolated from high temperature measurements [15] ( $D = 1.3 \times 10^{-15}$  cm<sup>2</sup>/s). Let us recall that this later measurements have been obtained from X-ray diffraction analysis at high temperature which is not considered as an accurate technique for diffusion coefficients determination. Our technique can be considered more accurate.

The LEED observations carried out at RT at the end of the dissolution process exhibit a sharp  $p(1 \times 1)$  LEED pattern in agreement with the recovery of a clean silver surface.

After deposition of one aluminum ML, the sample is then exposed to O<sub>2</sub> at  $4.10^{-6}$  Torr for 13 min at RT.

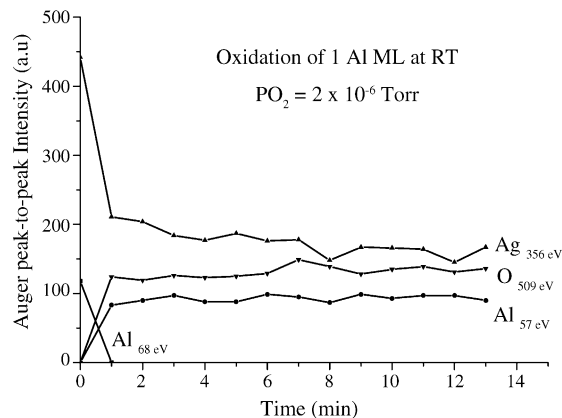


Fig. 3. Time dependence of the Auger peak-to-peak intensities during the oxidation process at RT.

The surface is controlled by AES during the oxidation process. The evolution of the surface composition during the sample exposition to the oxygen gas is shown on Fig. 3. Very rapidly, while an oxygen peak (509 eV) appears, a decrease of the silver peak (60%) is observed and, simultaneously, the aluminum peak is modified in intensity, shape and position. Fig. 4 shows more clearly the evolution of the aluminum peak due to the oxidation process.

As expected, the aluminum peak shifts to a lower energy from 68 to 57 eV. This value is quite far from that obtained for the surface of stoichiometric alumina (54 eV) which means that the oxide formed this way is not bulk alumina (Al<sub>2</sub>O<sub>3</sub>). Note also that all the

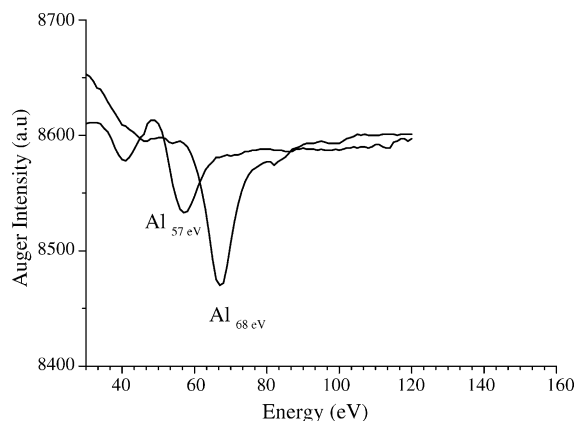


Fig. 4. The evolution of the Auger aluminum peak due to the oxidation process at RT.

aluminum has been oxidized since the aluminum peak at 68 eV has completely disappeared.

We also observe that the intensity of the aluminum peak drastically decreases (38%) as well as the silver peak. The fact that both Auger intensities of aluminum and silver decrease, suggest that the composition profile of the surface oxide layer corresponds to the sequence  $\dots/\text{Ag}/\text{Ag}/\text{Al}/\text{O}$  and not  $\dots/\text{Ag}/\text{Ag}/\text{O}/\text{Al}$  or  $\dots/\text{Ag}/\text{Ag}/(\text{Al}-\text{O})$ , i.e. a stack with an  $\text{AlO}_x$  bilayer made of one oxygen layer on top of the aluminum layer. The large attenuation of both aluminum and silver Auger signals, due to the oxidation process, suggests that  $x$  is probably close to one. This model is very close to the one proposed by Manabu Kiguchi et al. [16], concerning the growth of  $\text{MgO}$  on  $\text{Ag}(0\ 0\ 1)$  using the same procedure.

The strong silver attenuation could also suggest an oxidation at both sides of the Al layer. Nevertheless we think that an interface  $\text{Ag}-\text{O}$  is not possible, because silver does not oxidise at room temperature. We have checked that there is no oxidation of the pure silver surface at the oxygen pressure used here ( $2 \times 10^{-6}$  Torr) at RT. Only XPS measurements could settle this open question.

The thickness “ $d$ ” of this  $\text{AlO}_x$  compound can be estimated from the same equation previously used [12] using the same inelastic mean free path. The total Auger signal attenuation of silver (76%) gives an oxide thickness of about  $d = 7.9 \pm 0.2$  Å.

Furthermore it is important to notice that the oxidation process is very rapid since the evolution of the aluminum Auger peak (intensity and energy) is observed only 1 min after exposing the surface to the oxygen gas. After this first stage there is no more evolution of the Auger spectrum.

In order to check the stability of this superficial oxide we annealed the sample up to 500 °C in UHV conditions for 15 min and no major change in the Auger spectrum was observed. The only noticeable change was a shift of the aluminum peak from 57 to 56 eV. This behavior clearly shows the surprising thermal stability of this superficial oxide since there is no dissolution or evaporation of aluminum and/or oxygen atoms at elevated temperature. The oxidation process stabilizes the aluminum atoms at the surface forming a stable  $\text{AlO}_x$  compound. This  $\text{AlO}_x$  compound could form a diffusion barrier and probably a passivation layer for Ag. The shift observed after

annealing means that the annealing could slightly change the nature of the oxide.

These experimental results show that the superficial oxide ( $\text{AlO}_x$ ) which is obtained after oxidation at RT of one aluminum ML is not bulk alumina ( $\text{Al}_2\text{O}_3$ ). The near surface composition profile is probably  $\dots/\text{Ag}/\text{Ag}/\text{Al}/\text{O}$ . This superficial oxide is thermally stable: no dissolution process of both aluminum and oxygen atoms is observed at least up to 500 °C. This superficial oxide could be a diffusion barrier which could passivate the Ag substrate.

### Acknowledgements

The authors gratefully acknowledge F.A. d’Avitaya, L. Ravel and J. Bernardini for fruitful discussions. Financial support from the ST-Microelectronics is gratefully acknowledged. The CRMN is also associated with the Universities of Aix-Marseille II and III.

### References

- [1] H.J. Freund, E. Umbach, Adsorption of Ordered Surfaces of Ionic Solids and Thin films, Springer, Heidelberg, 1993.
- [2] J.S. Moodera, L.R. Kinder, J. Appl. Phys. 79 (1996) 4724.
- [3] Scott A. Chambers, Surf. Sci. Rep. 39 (2000) 105.
- [4] R. Franchy, Surf. Sci. Rep. 38 (2000) 195.
- [5] J.H. Park, G.S. Lee, J.Y. Yang, K.S. Yoon, C.O. Kim, J.P. Hong, H.J. Kim, Appl. Phys. Lett. 80 (2002) 3982.
- [6] V. Rose, V. Podgursky, I. Costina, R. Franchy, Surf. Sci. 541 (2003) 128.
- [7] Klaus, Shröder (Eds.), CRC Handbook of Electrical Resistivities of Binary Metallic Alloys, Chemical Rubber, Boca Raton, FL, 1983, p. 44.
- [8] T.L. Alford, D. Adams, T. Laursen, B.M. Ullrich, Appl. Phys. Lett. 68 (1996) 23.
- [9] W. Wang, W.I. Lanford, S.P. Murarka, Appl. Phys. Lett. 68 (1996) 12.
- [10] Gerald F. Malgas, Daniel. Adams, Phucanh. Nguyen, Yu. Wang, T.L. Alford, J.W. Mayer, Appl. Phys. Lett. 90 (2001) 11.
- [11] Y. Wang, T.L. Alford, Appl. Phys. Lett. 74 (1999) 1.
- [12] A. Barbier, Surf. Sci. 406 (1998) 69.
- [13] C. Léandri, H. Saifi, O. Guillermet, B. Aufray, Appl. Surf. Sci. 177 (2001) 303.
- [14] T.B. Massalski, Binary Alloy Phase Diagrams, 2nd ed., The Material Society, 1992.
- [15] Landolt, Börnstein, Tome 2, Diffusion in festen metallen und legierungen, 1990.
- [16] M. Kiguchi, S. Entani, K. Saiki, T. Goto, A. Koma, Phys. Rev. B 68 (2003) 115402.